Eur. Phys. J. B (2017) 90: 25
DOI: 10.1140/epjb/e2016-70472-0

THE EUROPEAN PHYSICAL JOURNAL B

Regular Article

Minimal dynamical description of eye movements

Juan I. Specht[1], Leonardo Dimieri[2,4], Eugenio Urdapilleta[3,4], and Gustavo Gasaneo[1,4,a]

[1] Departamento de Física, Universidad Nacional del Sur – IFISUR, Bahía Blanca (8000), Buenos Aires, Argentina
[2] Instituto de Investigaciones en Ingeniería Eléctrica – IIIE, UNS, CONICET Bahía Blanca (8000), Buenos Aires, Argentina
[3] División de Física Estadística e Interdisciplinaria, Centro Atómico Bariloche, S. C. de Bariloche (8400), Río Negro, Argentina
[4] Consejo Nacional de Investigaciones Científicas y Técnicas, CONICET, Buenos Aires, Argentina

Received 8 August 2016 / Received in final form 25 November 2016
Published online 1 February 2017 – © EDP Sciences, Società Italiana di Fisica, Springer-Verlag 2017

Abstract. In this paper we have addressed the question of whether a simple set of functions being the solution of a model, namely the damped harmonic oscillator with a general driving force, can satisfactorily describe data corresponding to ocular movements produced during a visual search task. Taking advantage of its mathematical tractability, we first focused on the simplest driving force compatible to the experimental data, a step-like activation. Under this hypothesis we were able to further simplify the system, once data from several experiments were fitted, producing an essentially parameter-free model that we plan to use in future applications. To increase the quality of the description of individual movements, we expanded the complexity in the forcing term and solved the inverse problem by using a proper mathematical formalism. Furthermore, additional terms, those arising from ocular drift and tremor, may be included within the same mathematical approach.

1 Introduction

The human being's eye is a highly refined bio-mechanical device. From the physical point of view, it is basically an almost spherical rigid body interacting with six very specialized dynamical belts. All possible ocular movements are regulated by the activities of the muscles bound to the sphere and by the damping produced by the septum around the eye. For static head and body conditions, eye movements associated to gaze shifting are classified into different categories depending on different sensory characteristics and possibly, differences in the subsystems subserving motor commands [1]. Smooth pursuit is the gaze allocation to moving objects, which requires an estimation of the object motion and the computation of the future projection of the gaze in order to keep the object on the fovea, where the eye has maximum resolution. Vergence is the coordinated movement of both eyes produced to keep a target in depth on focus. Finally, saccades are fast rotational movements used by the brain to bring to the fovea a relevant part of a fixed visual scene. These movements are considerably different from the smooth pursuit, as saccades are essentially sudden jumps in the position of the eye which moves the center of the fovea from one place to another. Closely related to the saccades are the microsaccadic movements, which are tiny rotations of the eye around a given point in the visual space [2]. In some extent arbitrary, these movements are assumed to be smaller than one sexagesimal degree. Both saccades and microsaccades are conjugated, e.g. they occur at the same time and same direction in both eyes.

According to recent studies, saccadic and microsaccadic movements share several characteristics and, in fact, there has been a long debate in literature whether saccadic and microsaccadic movements are different phenomena or not [3]. Based on their physical behavior, there seems to be no difference from one another and, furthermore, both may have the same neural substrate [4,5]. Importantly, the classification of different movements according to their amplitude has an impact on their projection on the retina. While microsaccadic movements are regularly associated to displacements of the center of the pupil on the order of dozens to hundreds of photo-receptors, larger saccadic movements range from hundreds to thousands [3]. Given that retinal ganglion cells, the only output from retina to cortex, have small receptive fields on the fovea [6], the same or different cells may be activated between events according to one or another type of movement.

Functionally, saccadic movements are associated to the exploration of large portions of the visual field, while microsaccades are linked to the exploratory behavior in a much smaller region of interest [7]. In view of this functional equivalence, it seems to be natural to consider both movements as a single phenomenon with a variable size [4,5]. Functionally, there is another reason why microsaccades are important. When fixating, visual adaptation fade out those portions that do not change their luminosity in time. Apparently, to avoid this, microsaccades

[a] e-mail: ggasaneo@gmail.com

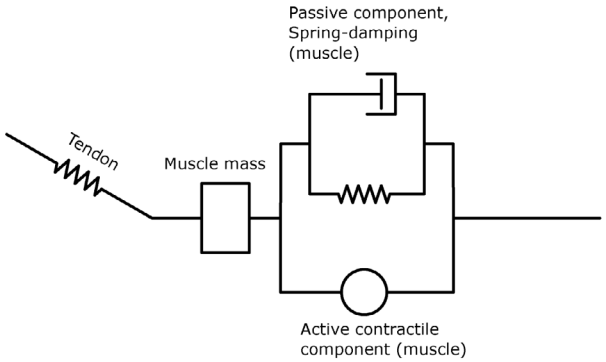

Fig. 1. Simple model of the eye. Muscle dynamics, consisting of an active force generator and a parallel passive damping, is in series to a nonlinear tendon.

bring a new set of photo-receptors to the light projection and thus, counteract visual fading [3,8–11]. In addition, microsaccades may be influenced by neural fluctuations. But, in this sense, two other types of tiny movements are continuously active, with completely different sizes and characteristics [12,13]. On the one hand, drift is a small-sized displacement with a much smaller velocity than saccadic-type movements. Drift can be originated from the imbalance of the action of the complementary muscles of the eye and it can be considered at some extent spurious, but also effective to prevent fading. On the other hand, the smallest of all the movements is the tremor, which is a high-frequency oscillatory eye rotation and its size corresponds to a displacement of the light projection in about a single photo-receptor [12,13].

All the movements described above are produced by the same set of muscles and commanded by the brain. A series of models designed to describe them separately has been proposed [14–18]. Modeling the eye movements implies to quantitatively characterize muscles, tendons, the ocular globe and all the constraints that they have. Also, it requires to describe neural activation and how neural innervation is connected to the muscle fibers. Perhaps the simplest way of representing the system is by considering the muscle as a mass-spring-damper ensemble in parallel with an neural active force, which is schematically depicted in Figure 1 (see Ref. [14]). In this simple model, the tendon is represented by a nonlinear elastic element in series to the muscle. A more elaborate model has been proposed by Enderle et al. [19–21], in which the muscle is considered to be arranged by summing up many units similar to that in Figure 1. This type of models attempts to physically describe the dynamics of the eye and the muscles associated in great detail and, naturally, they depend on a large set of parameters to be adjusted after solving a large set of ordinary differential equations.

With a completely different approach, very recently, Bettenbühl et al. [22] introduced a way to mathematically represent the structure of the eye displacements corresponding to saccades, including microsaccades, using the method of principal components. This approach showed to be very efficient because with two parameters the authors were able to faithfully describe the shape and magnitude of the saccades. One of the functions obtained was associated to the jump observed in the saccade and the second component was related to what is known as overshoot. Physically, these two characteristics of the eye movement are not separated. In this sense, the functions obtained with the principal components method are a very efficient phenomenological description, but it can not be directly associated with the physical processes supporting the real eye system. Additionally, data fitting is required a priori to define each component and therefore, this approach can not be considered as a predictive model. Besides, the authors also introduce a novel methodology to identify the occurrence of saccadic movements, including microsaccades, by the use of wavelet transform. They recognized that due to the abrupt nature of saccadic movements, the change in the position of the eye can be associated to a step function whereas its derivative, the velocity, can be related to a Dirac delta function. Wavelet transform is performed on finite time windows, and the singularities corresponding to jumps in the ocular position are identified as high frequency events. No discussion was presented in relation to a model representation for the drift or tremor.

In this work we aim to combine both approaches to describe the variations in the eye positions observed in eye-tracking data. On the one hand, following the mechanistic approach of detailed models, but considering the simplest minimal system preserving intrinsic processes, we present a description based on a driven harmonic oscillator. In this model, driving terms representing the neural activations essentially produce all possible movements. Temporal profiles of eye displacements are shaped by the oscillator frequency, the magnitude of the damping, and the time-course of neural activations. Data obtained from the eye-tracker is processed by a custom-defined algorithm to detect saccades, including microsaccades, and each jump is decomposed in terms of functions representing specific contributions in the forced mass-spring-damper system, which act as a sort of universal basis for the eye dynamics. In detail, the shape of the saccadic movements is projected on quasi-sturmian functions, which were introduced by Del Punta and co-workers in the context of atomic physics [23]. These functions, which are the solutions of a specific non-homogeneous equation with different forcing terms, form a complete basis set that incorporates the particular physics of the problem under consideration. This method can be naturally extended to include tremor and drift movements. On the other hand, even when this dynamical model remains tractable up to any order (which is useful to deal with the inverse problem of estimating neural activations from ocular movements), following the phenomenological approach of [22], next we focus on obtaining a minimal effective description, here constrained by considering a specific neural activation. Whereas in [22] any saccadic movement is essentially projected on two principal components, here the system dynamics produces these components with a proper combination of system parameters. Under this hypothesis of a simple step-like driving term, the dynamical model exhibits a concise solution, amenable for a fast estimation of parameters. Taking advantage of this fact, from the evaluation of thousands of

Fig. 2. Example of the visual search task. One of the pairs of images used for the experiment, with 10 s of the eye tracking recording data superimposed on the scene, as observed from the subject's point of view. Micro-movements during a relatively quiet fixation period is zoomed in at the top encircled panel.

saccadic movements we are able to infer specific relationships that further simplifies the dynamical description.

The organization of the paper is as follows. In Section 2 we describe the experiment performed to collect data corresponding to eye movements. A general characterization of the different types of movements is included. A custom-made procedure to detect the occurrence of saccadic movements of any magnitude from the data is also discussed. In Section 3 we describe the model used to fit the data. Saccades, drift and tremor will be discussed separately. In Section 4 we present a general discussion about the results obtained with the proposed methodology, including also a possible application of the model and the results obtained here.

2 Experiment

All data for this work was gathered from recordings of human eye movements using a SR-Research EyeLink 1000 eye-tracking device, with sample rate of 1000 Hz. To deliver and control the experiment, a custom-made code was developed in MATLAB 2007 with PsychToolBox installed. Subjects were 13 males and 7 females, matched in age (range: 20–40 years old). They were students or researchers with different academic backgrounds, randomly selected from the Universidad Nacional del Sur, where the authors of this contribution ran the experiments.

To produce a large dataset for modeling purposes, our goal when designing the visual experiment was to gather as many saccadic and microsaccadic movements as possible. For this reason, our setup resembles the one described by Otero-Millan et al. [4], where a paradigm of searching for differences produces a large number of saccades and microsaccades. Displacements due to tremor are in the order of magnitude of the eye-tracker's error, so its characterization results inaccurate. On the other hand, the long records produced in our experiments enable us to properly describe drift movements between jumps.

In detail, the experiment consisted of two almost identical images next to each other, where some differences were included in one of the images in order to boost visual search. Eight sets of two natural images as described were presented to each subject for a time period of one minute each. The complete sequence was repeated several times, totalizing an overall recording time between ∼8 min and ∼160 min for individual participants. The task consisted of exploring to find the differences and, due to the arrangement on the screen of these two images, large horizontal movements were induced. For the experiment, subjects rested their heads on a head support, at a distance of 78 cm from a monitor 44 cm wide and 25 cm high. The angular displacement between the centers of each image was ∼16 deg. In Figure 2 we show a sample of one of the pairs of images used. Superimposed to the images is the trace of the gaze during an interval of 10 s.

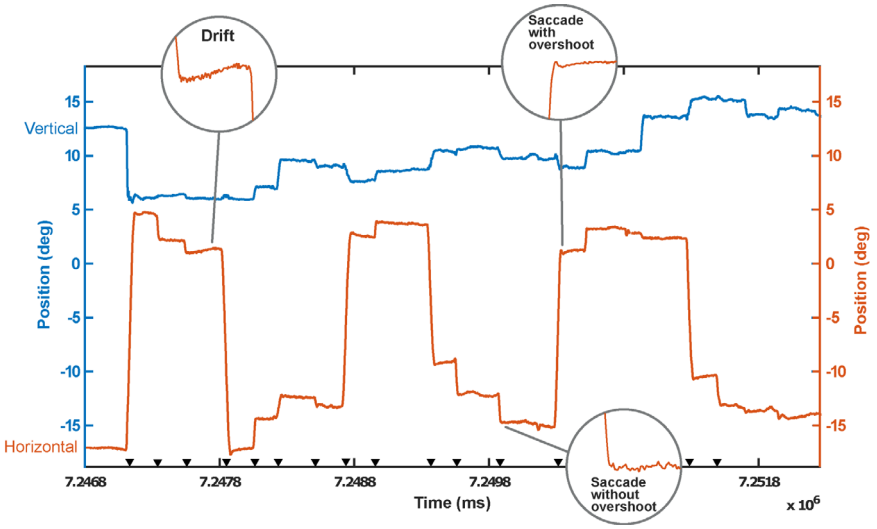

Fig. 3. A typical eye-tracking recording, decomposed in canonical directions, whose axis are arranged on left and right margins, respectively. Detailed zooms on particular events are displayed by encircled traces. Saccadic movements detected with the custom-made algorithm are indicated by arrows at the bottom.

2.1 Physical characteristics of saccadic, microsaccadic, drift, and tremor movements

In this section we summarize some features exhibited by different ocular movements during search and fixation. A typical eye-tracking recording is shown in Figure 3, where the horizontal and vertical angular displacements are displayed as a function of time.

Due to the particular design of the visual task, horizontal displacements are much larger than vertical ones, see respective scales in Figure 3. As identified by arrows on the temporal axis, the first and most significative structure in the data is the presence of large jumps in the horizontal position. After the jumps and for a while, the eye position remains more or less stable; those periods are the fixations. During these fixations, see Figure 3, we can observe the presence of small ascending or descending trends in the position; these ramp-like modulations are identified as drift movements. Finally, continuous high-frequency small fluctuations known as tremor, with amplitudes in the order of 6″ to 30″ of angular displacement and frequencies around 40 to 100 Hz, are superimposed to the previous movements. In our case, the eye-tracker we utilized was unable to resolve tremor accurately. The tiny oscillations observed in Figure 3 correspond to the noise generated by the eye-tracker itself.

Also in Figure 3 we show in more detail some of the jumps appearing in the horizontal movements. Here, we can notice the structure following an ascending or descending jump (i.e. to the right or to the left). Remarkably, different behaviors in the overshoot can be observed. All the structures appearing in the data provided by the eye-tracker are related to the physical characteristics of the eyes, i.e. the size, the mass and the inertia moment of the eye ball, the elastic and damping properties of the muscles attached to the ball, the damping properties of the septum supporting the eye ball, and to the neural activations that command the movements. Irrespectively of all the constitutive details of the eye system and the neural activations, our aim is to describe the system with a mathematically tractable simplified model, appropriate to describe data provided by the eye-tracker, i.e. a set of equations that allow us to generate movements similar to those performed by the eyes, with particular emphasis in saccades and microsaccades. The first fundamental task in order to accomplish this objective is to reliably identify the time at which jumps occur.

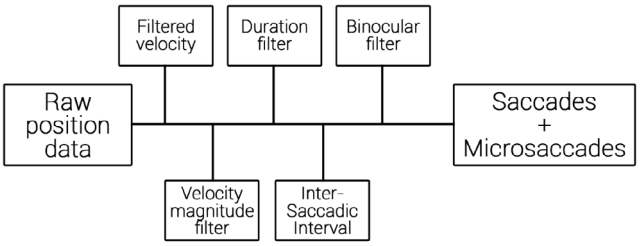

Fig. 4. Implementation of sequential filtering for detection of saccades and microsaccades.

2.2 Saccades and microsaccades detection

Saccadic and microsaccadic movements were detected according to a custom-made algorithm, based on ideas introduced by Engbert and Kliegl [24]. The code was written in MATLAB language, as an open package for online sharing and distribution[1]. In our algorithm, we use a set of ordered filters that sequentially analyze and refine detection of saccades and microsaccades from data (see Fig. 4).

In detail, the algorithm processes raw position data by first calculating the velocity of the eye movements.

[1] http://www.neufisur.uns.edu.ar/

Since all recordings are spuriously contaminated with high frequency background noise, and this noise is greatly amplified with the simple two-points derivative, we computed velocity within a Bartlett window of seven points, a procedure that minimizes noise contribution. In order to discard small spurious movements that can still be driven by noise, a minimum threshold value was used in the velocity data. Following, a filter on the temporal length of selected events is applied. Since saccadic and microsaccadic movements occur in a finite time interval, all movements having smaller durations than a minimum threshold are disregarded. Next, a condition on the inter-saccadic interval is considered. When a saccade or a microsaccade is produced, then there is a refractory period during which the generation of another movement is strongly inhibited. For the type of visual tasks considered here, the inter-saccadic interval is ∼200 ms on average, no matter whether the events are saccadic or microsaccadic movements. To filter out spurious movements, selected events were conditioned to fulfill a minimum inter-saccadic interval of 150 ms. Otherwise, the posterior event defining the interval is disregarded. Finally, selected events were restricted to be conjugate in order to be labelled as saccadic or microsaccadic movements. In detail, events produced from separate streams corresponding to movements on both eyes are confronted to each other. When temporal overlap between events in both streams is observed, then a saccade or microsaccade is finally declared.

3 Theoretical description

3.1 Driven harmonic oscillator representation for eye movements

As mentioned in the introduction, our main interest is to show that all structures observed in eye movements can be represented by a driven harmonic oscillator:

$$\left[\frac{d^2}{dt^2} + 2\gamma\frac{d}{dt} + \omega_0^2\right] X(t) = \mathcal{F}_s(t) + \mathcal{F}_t(t) + \mathcal{F}_d(t), \quad (1)$$

where X represents the angular position of a given coordinate (for example, the horizontal direction), $\gamma = k_v/J$ where k_v is the strength of a generic damping force and J is a representative moment of inertia of the eye-ball, $\omega_0^2 = k_e/J$ is the squared natural frequency of the system, where k_e is the strength of the restoring spring. The driving force $\mathcal{F}(t)$, in equation (1), was separated in three terms: the saccadic $\mathcal{F}_s(t)$, the tremor $\mathcal{F}_t(t)$, and the drift $\mathcal{F}_d(t)$ contributions. We will show that simple force models for each type of movement can be used to globally describe eye position changes.

The general solution of an inhomogeneous equation is the sum of two functions: $X_h(t)$, the solution of the homogeneous associated equation, and $X_p(t)$, the particular solution satisfying the non-homogeneity:

$$X(t) = X_h(t) + X_p(t). \quad (2)$$

The solution of the homogeneous equation

$$\left[\frac{d^2}{dt^2} + 2\gamma\frac{d}{dt} + \omega_0^2\right] X_h(t) = 0, \quad (3)$$

reads

$$X_h(t) = e^{-\gamma t}\left[A\cos(\Omega t) + B\sin(\Omega t)\right], \quad (4)$$

where $\Omega = \sqrt{\omega_0^2 - \gamma^2}$. A and B are coefficients to be determined by given initial conditions.

The particular solution $X_p(t)$ can be separated into three individual contributions:

$$X_p(t) = X_s(t) + X_t(t) + X_d(t), \quad (5)$$

accounting individually for each of the movements performed by the eyes (s: saccadic, t: tremor, d: drift). Each of these terms satisfies an equation identical to equation (1), where the right-hand side only includes the corresponding force. In the following subsections we will study each of them separately.

3.2 Description of saccadic and microsaccadic movements

In Figure 3 we can notice that saccadic movements are sudden jumps between two fixated points. Different behaviors can be observed after the jumps. In some cases, the final position X_f is reached after an overshoot with oscillations. In others, the final position is reached smoothly.

To analyze such different behaviors, we focused on two levels of descriptions, with different degree of sophistication. On the one hand, we focus on the simplest driving force compatible with the observed data: $\mathcal{F}_s(t)$ as a time-step function with proper initial and final values. This model will provide valuable information about parameters of the dynamics. On the other hand, more complex models can be derived by increasing the accuracy of the description of $\mathcal{F}_s(t)$. In particular, we will show that its representation in a proper basis set rapidly produces very satisfactory results when fitting saccadic movements.

3.2.1 Step driving force

To model saccades and microsaccades we start with the simplest possible representation of $\mathcal{F}_s(t)$, which corresponds to a step:

$$\mathcal{F}_s(t) = \begin{cases} 0, & t < t_i \\ f_{s0}, & t \geq t_i, \end{cases} \quad (6)$$

where f_{s0} is a constant. To consider the effect of this force, let's suppose that the horizontal position of the eye at times $t < t_i$ is stationary, and denoted by X_i. For $t \geq t_i$, movement is governed by

$$\left[\frac{d^2}{dt^2} + 2\gamma\frac{d}{dt} + \omega_0^2\right] X_s(t) = f_{s0}, \quad (7)$$

whose solution reads

$$X_s(t) = \frac{f_{s0}}{\omega_0^2} + e^{-\gamma(t-t_i)} \times \left[A_s \cos\left(\Omega(t-t_i)\right) + B_s \sin\left(\Omega(t-t_i)\right)\right]. \quad (8)$$

The effect of this force is to move the mass from the initial position $X_s(t = t_i) = X_i$ to the final position $X_s(t = t_f) = X_f$, after performing (or not) damped oscillations produced by the spring and the absorber. At the initial position the mass is at rest, $\dot{X}_s(t = t_i) = 0$. All these considerations allow us to determine f_{s0}, A_s and B_s. At $t = t_i$ we have

$$X_s(t = t_i) = X_i = \frac{f_{s0}}{\omega_0^2} + A_s, \quad (9)$$

and

$$\dot{X}_s(t = t_i) = 0 = -\gamma\ A_s + \Omega\ B_s. \quad (10)$$

On the other hand, when the effects of the stabilization finish, at $t = t_f$, the eye ends up at the final position, imposing the following condition

$$X_s(t = t_f) = X_f = \frac{f_{s0}}{\omega_0^2}. \quad (11)$$

Thus, finally:

$$f_{s0} = \omega_0^2\ X_f, \quad (12)$$

$$A_s = X_i - \frac{f_{s0}}{\omega_0^2}, \quad (13)$$

$$B_s = \frac{\gamma}{\Omega}\ A_s. \quad (14)$$

In consequence, the final expression for the position of the harmonic oscillator driven by a step function is

$$X_{step}(t) = X_f + (X_i - X_f)\, e^{-\gamma(t-t_i)} \times \left[\cos\left(\Omega(t-t_i)\right) + \frac{\gamma}{\Omega}\sin\left(\Omega(t-t_i)\right)\right]. \quad (15)$$

The parameters γ and ω_0 can be optimized to represent, within this simple model, the data obtained from the eye-tracker, as shown in Figure 5.

When using this simple model we are assuming that a driven linear harmonic oscillator can globally represent the saccadic movements in the set of data collected with the eye tracker. In this sense, we are not pursuing the best mechanistic representation of ocular movements, but a phenomenological approach (with a physical interpretation) that allow us to *simulate* the observed movements. In this simple model, only two parameters are undetermined, ω_0 and γ, which provide certain global information about the elasticity and the damping of the ocular plant, and have to be evaluated by fitting data. In Figure 6 we plot the best fitting values of γ as a function of ω_0, for all saccadic movements detected for all participants. The very first observation is the linear relationship between both parameters, $\gamma = \mathcal{C}_s\ \omega_0$, for large saccades ($\geq\sim$3 deg), and the spread of values for small movements ($\leq\sim$3 deg). Interestingly, the same relation holds across participants.

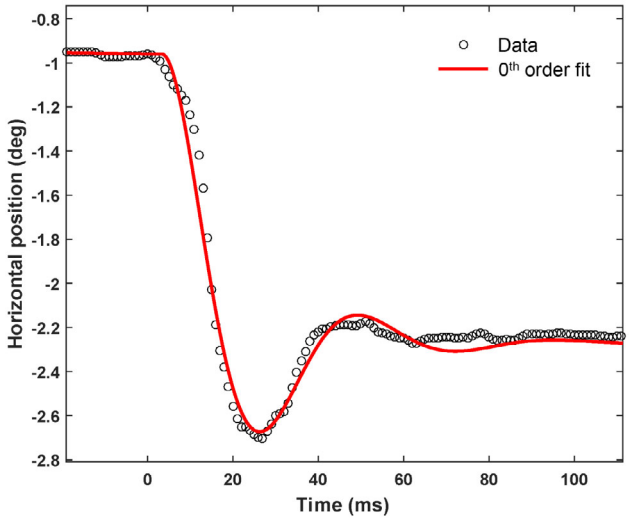

Fig. 5. Sample saccadic movement described with a harmonic oscillator model driven by a step function.

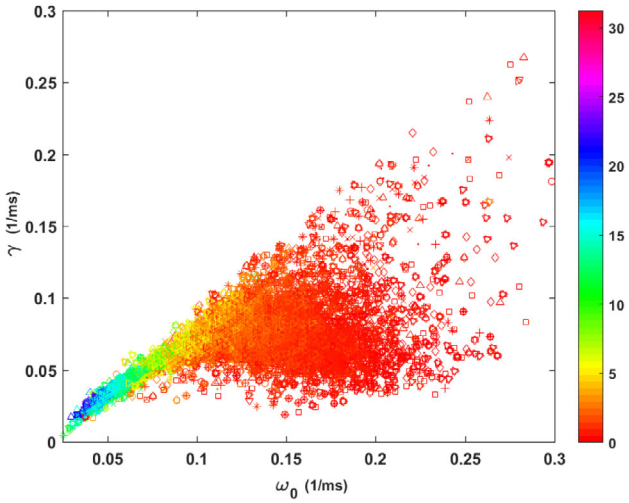

Fig. 6. Relation between the best fitting parameters γ and ω_0 obtained with the harmonic system driven by a step function, for all saccadic movements detected in the complete dataset (all participants). Saccade magnitude is represented by the color indicated at the right margin. Different symbols correspond to different participants.

These parameters are physically relevant and are associated to the real dynamics underlying saccade generation. They can be thought of as an alternative representation for the c_0 and c_1 obtained by Bettenbühl et al. using a principal components analysis [22]. In this case, different combinations of γ and ω_0 produce different temporal profiles in response to a step function, which is assumed in this subsection as the fundamental driving force. The only difference is that here, as shown above, both parameters show certain dependence on the magnitude of the saccade. This may be interpreted as one of the limitations of this simple model. However, by considering a more complex representation of the driving force, we may overcome

or reduce these limitations, which will be discussed in the following subsection.

To take advantage of the analytical tractability and explore the limits of the simple harmonic system driven by the step function, we will derive some useful relationships that have an experimental counterpart. From equation (15) we can calculate the velocity and the acceleration by taking the first and second derivatives with respect to time. When the velocity reaches the first maximum, the acceleration is zero (for the first time after the step). The time at which this situation occurs can be obtained analytically and replaced into the velocity definition, to obtain the peak velocity V_p:

$$V_p = (X_f - X_i)\ \omega_0 \times \exp\left\{-\frac{\gamma}{\sqrt{\omega_0^2-\gamma^2}}\arctan\left[\frac{\sqrt{\omega_0^2-\gamma^2}}{\gamma}\right]\right\}, \quad (16)$$

which depends linearly on the saccade magnitude, $X_f - X_i$. The multiplying factor depends both on γ and ω_0. However, if we use the linear relationship obtained before from the data fitting, the peak velocity reduces to

$$V_p = (X_f - X_i)\ \omega_0 \times \exp\left\{-\frac{\mathcal{C}_s}{\sqrt{1-\mathcal{C}_s^2}}\arctan\left[\frac{\sqrt{1-\mathcal{C}_s^2}}{\mathcal{C}_s}\right]\right\}. \quad (17)$$

As reported in references [4,25], peak velocity and amplitude of the saccades are linearly related in a log-log representation. The data collected in our experiments give the same behavior, see Figure 7a, in agreement with the main sequence reported in reference [25]. When plotting the data on linear scales our experiments present the relationship observed in Figure 7b. To keep the model as simple as possible, we can describe this dependence between both magnitudes by two different linear regimes, separated at amplitudes of ∼3 degrees. Defining the slopes of these two linear descriptions by $\mathcal{K}_1$ and $\mathcal{K}_2$, the multiplicative factor in the linear relationship between V_p and $(X_f - X_i)$ given by equation (17), implies that ω_0 is completely determined within each region,

$$\omega_{0,i} = \mathcal{K}_i \exp\left\{\frac{\mathcal{C}_s}{\sqrt{1-\mathcal{C}_s^2}}\arctan\left[\frac{\sqrt{1-\mathcal{C}_s^2}}{\mathcal{C}_s}\right]\right\} \quad \text{with} \quad i=1,2. \quad (18)$$

This simple model, then, can be used in these two different regimes by assessing individual $\mathcal{K}_i$ $(i = 1, 2)$. Within this approach, only a single free parameter completely determines a saccade, namely the saccade amplitude defined by X_i and X_f, without any further information.

3.2.2 Smooth driving force

In this section, we extend the model to include a more complex activation. In addition, by a proper analytical procedure we formalize the solution to the inverse problem, i.e. the determination of the neural activation commanding movements from data (of course, under the hypothesis and limitations of this particular system). Both, the increase of the complexity and the solution to the inverse problem, allow us to explore the limits of the linear representation.

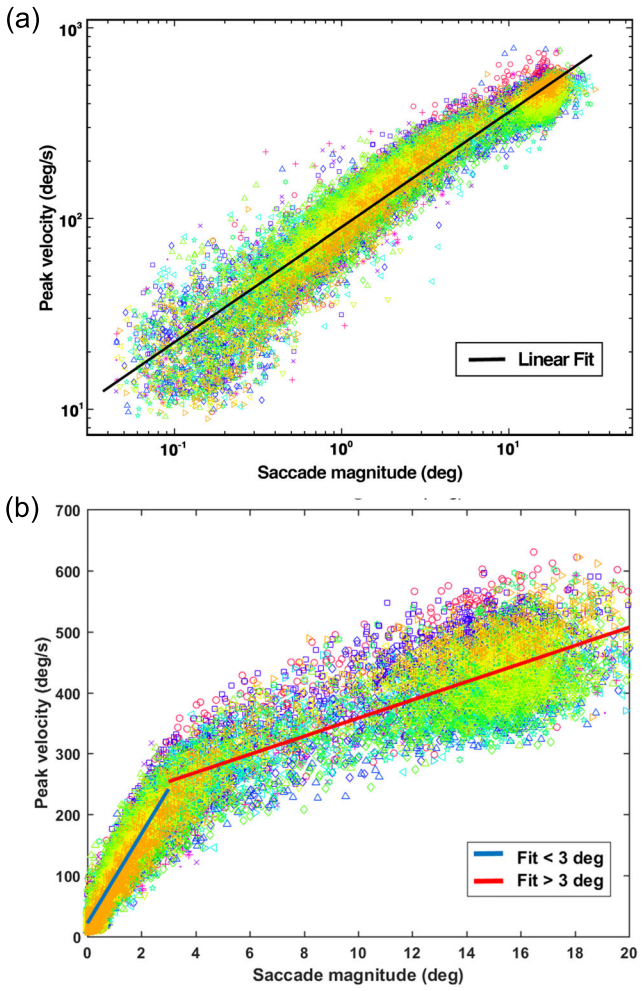

Fig. 7. Peak velocity as a function of the amplitude of the saccades. Data from different participants is represented by different symbols. In (a) we present the data in Log-Log scale, where a linear behavior is clearly observed, in agreement with literature [25]. In (b) we present the data in linear scales, as well aslinear fits on the different ranges considered.

To represent complex activations we use a convenient set of functions, triggered at time t_i:

$$\mathcal{F}_s(t) = f_{s0} + \sum_{n=1} f_{sn}\ F_n(\alpha, t)\ \ , \quad t \geq t_i. \quad (19)$$

The first term is just the contribution of the step function already discussed, which is considered the zeroth order term. The higher order term contributions, $n \geq 1$, allow us to represent more realistic neural activations. We will assume that the $\{F_n(\alpha, t)\}$ form a complete basis set of functions that could or could not be orthogonal. In such a way, any function can be expanded in this series representation with coefficients f_{sn} appropriately determined. Actually, there is no restriction and the sum can be equally turned into an integral, extending its mathematical generality.

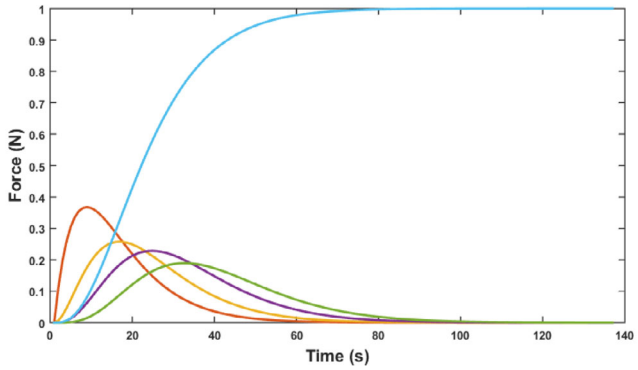

Fig. 8. Set of basis functions used to project saccadic activations. Red, orange, violet, and green lines are the four first terms of this series representation, respectively, whereas the cyan line corresponds to these four functions subtracted from the step activation.

Because of the linearity of the system, from the solution to the set of equations

$$\left[\frac{d^2}{dt^2} + 2\gamma\frac{d}{dt} + \omega_0^2\right] x_n(\alpha, t) = F_n(\alpha, t), \tag{20}$$

we can build the solution $X_s(t)$ to a generic driving force, given by equation (19), by superposition

$$X_s(t) = X_{step}(t) + \sum_{n=1} f_{sn}\; x_n\,(\alpha, t)\,. \tag{21}$$

As $\{F_n(\alpha, t)\}$ form a complete basis set, then $\{x_n(\alpha, t)\}$ has the same property and any function describing ocular movements can be expressed in this series representation. This set of functions is similar to the one recently discussed in reference [23] in the context of atomic physics.

To smooth the transition given by the abrupt step function imposed by the zeroth order, a very convenient set of basis functions is given by $F_n(\alpha, t) = t^{n-1}e^{-\alpha t}$, for $n \geq 1$. In Figure 8 we show the first 4 elements, as well as the function $1 - \left[1 + \alpha t + \frac{(\alpha t)^2}{2!} + \ldots\right] e^{-\alpha t}$. As observed, a smooth transition can be easily represented with a few terms within this set of basis functions.

To obtain the solutions $x_n(\alpha, t)$ of equation (20), we first solve the Green's associated function and then express $x_n(\alpha, t)$ as a convolution. Explicitly,

$$x_n(\alpha, t) = \frac{1}{\Omega}\int_{t_i}^{t} e^{-\gamma(t-t')}\sin\left[\Omega(t-t')\right] t^{n-1}e^{-\alpha t'}\,dt'. \tag{22}$$

The first order can be easily obtained by integration and reads

$$\begin{aligned} x_1(\alpha, t) = {} & \frac{e^{-\alpha t}}{\alpha^2 + \omega_0^2 - 2\alpha\gamma} \\ & - \frac{e^{-\alpha t_i}}{\alpha^2 + \omega_0^2 - 2\alpha\gamma} e^{-\gamma(t-t_i)} \\ & \times \left[\cos\left(\Omega(t-t_i)\right) + \frac{\gamma - \alpha}{\Omega}\sin\left(\Omega(t-t_i)\right)\right]. \end{aligned} \tag{23}$$

Instead of performing the integration in equation (22) to obtain the following terms, it is more convenient to proceed with a recursive scheme by taking derivatives with respect to α. For example, the solution to the case $n = 2$ reads,

$$\begin{aligned} x_2(\alpha, t) &= -\frac{dx_1(\alpha, t)}{d\alpha} \\ &= -\frac{1}{\Omega}\int_{t_i}^{t} e^{-\gamma(t-t')}\sin\left[\Omega(t-t')\right] t' e^{-\alpha t'}\,dt'. \end{aligned} \tag{24}$$

Since normally we only measure ocular movements, being neural activations intrinsic processes that remain unknown, here we devise a method to extract this information from measurements. Naturally, these inferred activations are only valid within the framework of the proposed dynamics. Assuming that $D_s(t)$ represents the movement during a saccadic event, thus according to equation (21), we can decompose it as

$$D_s(t) = X_{step}(t) + \sum_{n=1} d_n\; x_n\,(t)\,, \tag{25}$$

where we assume that the dynamical as well as the forcing parameters (ω_0, γ, and α) are already known. Since the step function is the only function that survives at large times, its explicit time-course can be independently evaluated and it is still given by equation (15). By subtracting the real movement from the step solution, we define

$$\tilde{D}_s(t) = D_s(t) - X_{step}(t) = \sum_{n=1} d_n\; x_n(t). \tag{26}$$

Projecting to the left with the functions x_n at both sides of equation (26), and performing an integration in the time interval where the saccadic motion occurs, we have

$$\int_{t_i}^{t_f} x_j(t)\;\tilde{D}_s(t)\;dt = \sum_{n=1} d_n\;\int_{t_i}^{t_f} x_j(t)\;x_n(t)\;dt. \tag{27}$$

Data for the saccadic motion $D_s(t)$, or its *deflection* $\tilde{D}_s(t)$, is obtained with the eye-tracker and it is given with a certain temporal resolution. In consequence, equation (27) should be performed numerically with standard integration methods. By defining coefficients

$$D_{s,j} = \int_{t_i}^{t_f} x_j(t)\;\tilde{D}_s(t)\;dt, \tag{28}$$

$$O_{jn} = \int_{t_i}^{t_f} x_j(t)\;x_n(t)\;dt, \tag{29}$$

then, equation (27) can be summarized as a vectorial equation

$$\mathbf{D}_s = \mathbb{O}\cdot\mathbf{d} \tag{30}$$

which, by simple inversion, builds a procedure for determining coefficients d_n

$$\mathbf{d} = \mathbb{O}^{-1}\cdot\mathbf{D}_s. \tag{31}$$

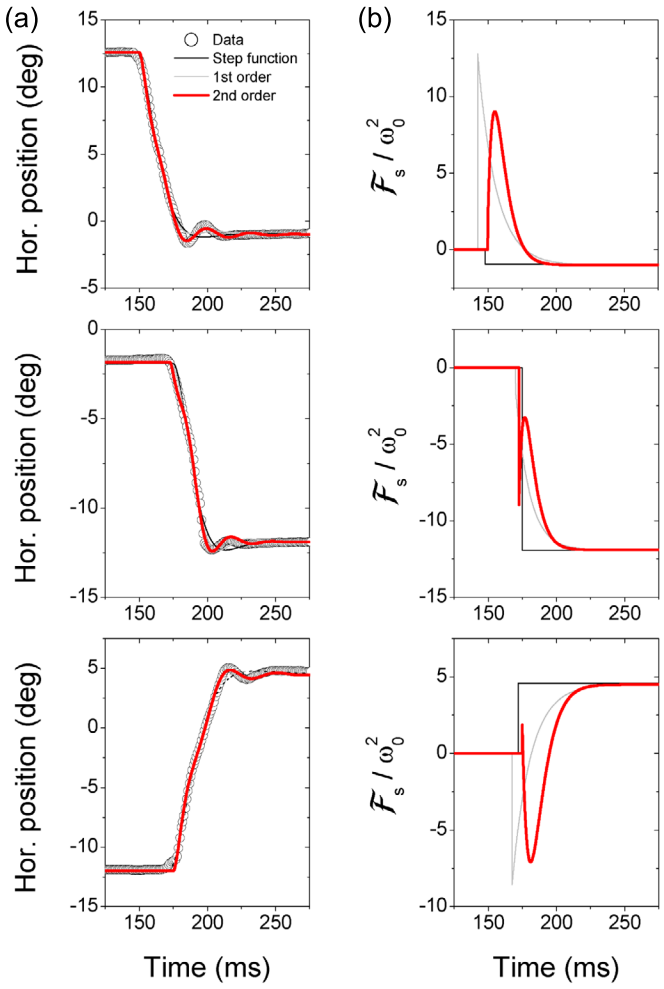

Fig. 9. Fit of saccadic movements with general activations. (a) Representative examples (black symbols), as well as theoretical descriptions up to different orders. Black, gray, and red continuous lines for forcing terms corresponding to a 0th, 1st and 2nd order series representations, respectively, fitted with the procedure described in the main text. Adjustable parameters were independent in each case (ω_0, γ, α, t_i). (b) Associated activations, for the best fitting at different orders.

Once coefficients d_n are obtained with the preceding methodology for the particular saccadic movement under analysis, its neuronal activation, within the framework of the harmonic driven model, is given by

$$\mathcal{F}_s(t) = \omega_0^2\ X_f + \sum_{n=1} d_n\ F_n(t), \quad t \geq t_i, \tag{32}$$

where $F_n(t)$ are the exponential basis functions defined previously, $F_n(t) = t^{n-1}e^{-\alpha t}$.

In Figures 9a and 9b we show some representative saccadic movements fitted with this methodology at different orders, and the associated activations, respectively. As observed, with only a few orders the saccadic movements are perfectly fitted.

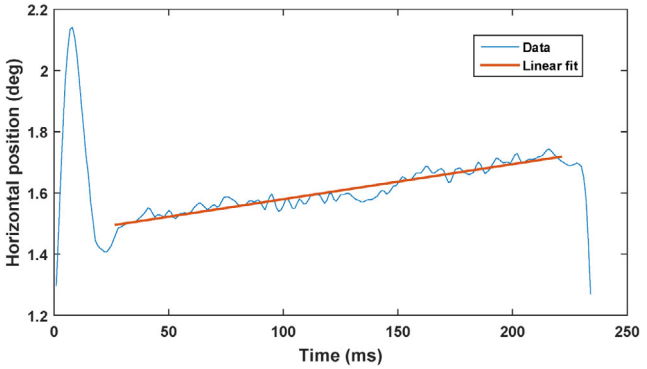

Fig. 10. A sample of drift, fitted with a linear function. As observed by the small slope of the fitted line, this type of movement is of very low velocity.

3.3 Drift

Different types of interpretation have been considered for the drift appearing during fixations [26–28]. Irrespective of its cause, the effect is that the fixated image is slowly moved across the retina, being the typical displacement of about a dozen of photo-receptors [13]. The data collected in our experiments show that the drift produces a displacement of, e.g., the horizontal position, that grows linearly in time, see Figure 10. This type of behavior appearing in the data can be easily represented by our simple driven harmonic model, equation (1).

As discussed in the previous subsection, saccades are produced by a force that rapidly grows from one constant value to another. Differently, drift appears as a temporally dependent non-constant force, which is continuously shifting the equilibrium position of a spring-mass-damper system. To generate this behavior, the force $\mathcal{F}_d(t)$ appearing in equation (1) has to read

$$\mathcal{F}_d(t) = A_d\ t. \tag{33}$$

The solution of equation (1) with the forcing imposed by $\mathcal{F}_d(t)$, given by equation (33), determines $X_d(t)$. This solution can be straightforwardly obtained from the Green's approach we previously presented, equation (22), considering the order two in the limit $\alpha \to 0$, i.e., by $X_d(t) = x_2(\alpha \to 0, t)$:

$$\begin{aligned}\frac{X_d(t)}{A_d} = &-\frac{2\gamma}{\omega_0^4} + \frac{t}{\omega_0^2} - \frac{t_i\ e^{-\gamma(t-t_i)}}{\omega_0^2}\Big[\cos\left(\Omega(t-t_i)\right) \\ &+ \frac{\gamma}{\Omega}\sin\left(\Omega(t-t_i)\right)\Big] \\ &+ \frac{e^{-\gamma(t-t_i)}}{\omega_0^4}\Big[2\gamma\cos\left(\Omega(t-t_i)\right) \\ &+ \left(\frac{2\gamma^2-\omega_0^2}{\Omega}\right)\sin\left(\Omega(t-t_i)\right)\Big].\end{aligned} \tag{34}$$

The values of γ and ω_0 are first determined by adjusting the saccades or microsaccades and then, the magnitude A_d may be evaluated in those cases where drift appears, see Figure 10.

3.4 Tremor

Tremor is associated to unavoidable noise, possibly caused by unbalanced tensions between the antagonist muscles [29]. Uncontrolled or random neural activity may produce an uncontrolled muscular activation which may be projected onto the eye movement as constant tremor. As mentioned in Section 2, the accuracy of the eye-tracker used here is not enough to properly record these very small vibrations. However, we will show how tremor can be included in our very simple model. For this purpose and as a general example, we introduce the following representation for $\mathcal{F}_t(t)$ [30]:

$$\mathcal{F}_t(t) = \frac{a_0}{2} + \sum_{n=1}^{\infty} \left[a_n \cos(n\,\Delta\omega\,t) + b_n \sin(n\,\Delta\omega\,t)\right]. \quad (35)$$

The coefficients are statistically independent, gaussian variables of mean value zero, and $\langle a_n^2\rangle = \langle b_n^2\rangle = w(n\,\Delta\omega)\Delta\omega$, where $w(\omega)$ is the spectral intensity of the noise. This representation of the noise turns accurate in the limit $\Delta\omega \to 0$.

With this driving force, the position of the eyes are governed by the equations:

$$\left[\frac{d^2}{dt^2} + 2\gamma\frac{d}{dt} + \omega_0^2\right] X_{tn}(t) = \left\{ \begin{array}{c} \frac{a_0}{2} \\ \cos(n\,\Delta\omega\,t) \\ \sin(n\,\Delta\omega\,t) \end{array} \right\}, \quad (36)$$

where brackets indicate a complete set of basis functions. The $X_{tn}(t)$ functions also form a complete basis set; they are quasi-sturmian functions, as those mentioned in the previous sections. They are related to the sturmian functions discussed recently by Rawitscher and Liss [31]. Given the fact that tremor is always present, the transient solution, given by the homogeneous part, decays as a consequence of the damping term. Then, the solution to consider for tremor is:

$$\begin{aligned} X_t(t) = {} & \frac{a_0}{2\omega_0^2} \\ & + \sum_{n=1}^{\infty} \frac{\left[\omega_0^2 - (n\,\Delta\omega)^2\right] a_n - 2\gamma\, n\,\Delta\omega\, b_n}{\left[\omega_0^2 - (n\,\Delta\omega)^2\right]^2 + (2\gamma\, n\,\Delta\omega)^2} \cos(n\,\Delta\omega\,t) \\ & + \sum_{n=1}^{\infty} \frac{\left[\omega_0^2 - (n\,\Delta\omega)^2\right] b_n + 2\gamma\, n\,\Delta\omega\, a_n}{\left[\omega_0^2 - (n\,\Delta\omega)^2\right]^2 + (2\gamma\, n\,\Delta\omega)^2} \sin(n\,\Delta\omega\,t). \end{aligned}$$

Here we considered a particular kind of noise, but this is not a limitation. Any type of noise can be included in the description of the general displacement of the eye using the function defined in equation (5), by taking into account a proper characterization.

4 Discussion

The main objective of the present contribution was to implement a method to represent, as easy and reliable as possible, the data resulting from eye tracking recordings. Different approaches based on numerical methods can be used to fit the data, as for example in the work of Bettenbühl et al. [22]. However, we aimed to describe ocular movements with a physical model, complex enough to capture the basic phenomena, but simple in order to bound mathematical complexity. Within this framework, we proposed a minimal model and a proper series representation, whose parameters can be globally fitted from a complete dataset produced under different conditions. The representation is essentially the solution to a damped harmonic oscillator driven by an arbitrary function. This simple description can be thought of as a lumped representation of all the relevant physics behind the eye movements (or, equivalently, it may be considered as a linear version of a nonlinear complex system as those proposed by Enderle and collaborators, see [19–21]), and for that reason turned to be efficient. When considering a complex activation, the parameters of the driving force were also used as fitting parameters [32]. As we showed, just two terms of the quasi-sturmian functions are enough to have a quite refined representation of the data.

In order to capture the minimal description of the dynamics behind saccadic movements, we considered a further simplification of the previous approach by assuming the simplest driving force compatible with eye tracking data, a step-like activation. Under this assumption, the natural frequency, the damping strength, and the initial and final conditions during each saccadic jump determine completely its dynamical behavior. The simple mathematical description of this approach enable us to compare thousands of saccadic events on the same grounds, namely the specific values of the parameters that best describe the temporal evolution of individual saccadic movements. As we showed by fitting a large dataset of saccadic movements, the simple picture of a damped harmonic oscillator driven by a step function leads to a systematic (effective) dependence between the natural frequency and the damping strength, which turns out to be linear in a given range of saccade magnitudes. This corresponds to horizontal movements larger than $\sim$3 deg. For smaller saccades, both parameters seem to scatter independently of each other. A further analysis of the peak velocity as a function of the saccadic magnitude revealed a general effective law relating the natural frequency with the initial and final horizontal positions. Obviously, intrinsic properties of the eye system can not be defined by the movement generated a posteriori. However, we wish to stress that, under the assumption of a step-like driving force, we produced an *effective* system which, with the relationships found, turned out to be a completely parameter-free model. In this sense, the model will produce a specific temporal profile that depends on the saccade magnitude, maybe failing in describing the finest details of the saccadic waveform, but compatible with a minimal dynamical representation.

During reading, a normal condition of a normal subject is to have a text at a given distance from the eyes. Motor commands produced by our brain, constrained by the oculomotor plant and the reading distance, is such that there are jumps from word to word (with skips) stopping

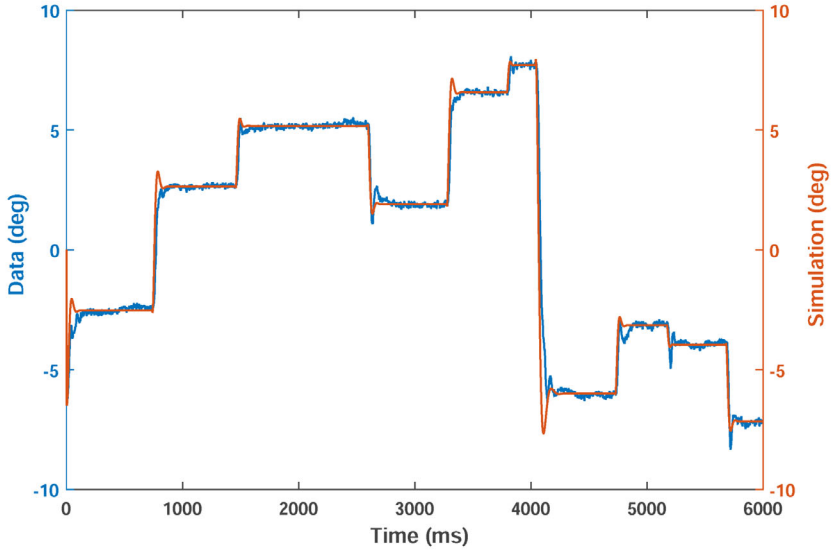

Fig. 11. Comparison of a recording obtained in a reading experiment (blue line) and a simulation (orange line) in which we used the previously obtained values for the parameters of the harmonic oscillator model.

on the center of mass of some of them. As reading goes, there are different times associated to different components of the reading process. There is a time involved in the intrinsic dynamics of the ocular plant, which is associated to the inertia of the system. Another time will be associated to the linguistic analysis of the information provided by the text and the particular word that it is being read. To proceed with the reading, the brain takes the decision of where to jump, how far from the current word, depending, for example, on the role of the word in the phrase. With this in mind, the model we proposed in this contribution is functional, on the one hand, to the idea of realistically reproducing the time associated to the dynamic inertia. On the other hand, we have a systematic procedure that generates the driving forces needed to predict the positions when reading. As a long term goal, we wish to consider a neural network that learns to predict reading by producing the proper activations on this simple harmonic oscillator based on the linguistic context and cognitive demands [15]. The network could learn to identify the occurrence of different words under different contexts and, by training, to select the parameters of the following jump according to the ongoing reading. In Figure 11 we show the data obtained while a person is reading a text. The conditions of the experiment were similar to those of the previous experiments. The size of the text was 60 pt on screen. We can see that our fitting function reproduce perfectly the positions and partially the shape of the saccades produced by the eye while the reading process takes place. As a continuation of the present work, we expect that by training a neural network that defines the driving term of the damped harmonic system we can reproduce the characteristics of reading a simple text.

We want to thank the support by PGI (24/F049) of the Universidad Nacional del Sur.

References

1. D.L. Sparks, Nat. Rev. Neurosci. **3**, 952 (2002)
2. M. Rolfs, Vision Res. **49**, 2415 (2009)
3. S. Martinez-Conde, J. Otero-Millan, S.L. Macknik, Nat. Rev. Neurosci. **14**, 83 (2013)
4. J. Otero-Millan, X.G. Troncoso, S.L. Macknik, I. Serrano-Pedraza, S. Martinez-Conde, J. Vision **8**, 1 (2008)
5. J. Otero-Millan, S.L. Macknik, A. Serra, R.J. Leigh, S. Martinez-Conde, Ann. N.Y. Acad. Sci. **1233**, 107 (2011)
6. L.J. Croner, E. Kaplan, Vision Res. **35**, 7 (1995)
7. J. Otero-Millan, S.L. Macknik, R.E. Langston, S. Martinez-Conde, Proc. Natl. Acad. Sci. USA **110**, 6175 (2013)
8. S. Martinez-Conde, S.L. Macknik, X.G. Troncoso, T.A. Dyar, Neuron **49**, 297 (2006)
9. M.B. McCamy, J. Otero-Millan, S.L. Macknik, Y. Yang, X.G. Troncoso, S.M. Baer, S.M. Crook, S. Martinez-Conde, J. Neurosci. **32**, 9194 (2012)
10. M.B. McCamy, S.L. Macknik, S. Martinez-Conde, J. Physiol. **592**, 4381 (2014)
11. F.M. Costela, M.B. McCamy, S.L. Macknik, J. Otero-Millan, S. Martinez-Conde, PeerJ **1**, e119 (2013)
12. S. Martinez-Conde, S.L. Macknik, J. Vision **8**, 1 (2008)
13. S. Martinez Conde, S.L. Macknik, D.H. Hubel, Nat. Rev. Neurosci. **5**, 229 (2004)
14. C.F. Martin, L. Schovanec, in *Dynamical Systems, Control, Coding, Computer Vision*, edited by G. Picci, D.S. Gilliam, Progress in Systems and Control Theory **25**, 173 (1999)
15. R. Engbert, J. Neurosci. **32**, 8035 (2012)
16. O. Komogortsev, C. Holland, S. Jayarathna, A. Karpov, ACM Trans. Appl. Percept. **10**, 27 (2013)
17. I.B. Wijayasinghe, Coordination and control of human eye and head: a classical mechanics approach, Ph.D. thesis, 2013
18. B.K. Ghosh, I.B. Wijayasinghe, S.D. Kahagalage, IEEE Access **2**, 316 (2014)
19. W. Zhou, X. Chen, J. Enderle, Int. J. Neural Syst. **19**, 309 (2009)

20. J.D. Enderle, W. Zhou, *Models of Horizontal Eye Movements. Part 2: A 3rd-Order Linear Saccade Model* (Morgan and Claypool Publishers, San Rafael, CA, 2010)
21. J.D. Enderle, D.A. Sierra, Int. J. Neural Syst. **23**, 1350002 (2013)
22. M. Bettenbühl, C. Paladini, K. Mergenthaler, R. Kliegl, R. Engbert, M. Holschneider, J. Eye Mov. Res. **3**, 1 (2010)
23. J.A. Del Punta, M.J. Ambrosio, G. Gasaneo, S.A. Zaytsev, L.U. Ancarani, J. Math. Phys. **55**, 052101 (2014)
24. R. Engbert, R. Kliegl, Vision Res. **43**, 1035 (2003)
25. A.T. Bahill, M.R. Clark, L. Stark, Math. Biosci. **24**, 191 (1975)
26. L. Matin, E. Matin, D.G. Pearce, Vision Res. **10**, 837 (1970)
27. J.-R. Liang, S. Moshel, A.Z. Zivotofsky, A. Caspi, R. Engbert, R. Kliegl, S. Havlin, Phys. Rev. E **71**, 031909 (2005)
28. K. Mergenthaler, R. Engbert, Phys. Rev. Lett. **98**, 138104 (2007)
29. R.H.S. Carpenter, *Movements of the eyes*, 2nd. edn. (Pion, London, 1988)
30. N.M. Blachman, Information and Control **1**, 56 (1957)
31. G. Rawitscher, J. Liss, Am. J. Phys. **79**, 417 (2011)
32. D.M. Mitnik, F.D. Colavecchia, G. Gasaneo, J.M. Randazzo, Comp. Phys. Commun. **182**, 1145 (2011)